

# NJC

Accepted Manuscript



This is an *Accepted Manuscript*, which has been through the Royal Society of Chemistry peer review process and has been accepted for publication.

*Accepted Manuscripts* are published online shortly after acceptance, before technical editing, formatting and proof reading. Using this free service, authors can make their results available to the community, in citable form, before we publish the edited article. We will replace this *Accepted Manuscript* with the edited and formatted *Advance Article* as soon as it is available.

You can find more information about *Accepted Manuscripts* in the [Information for Authors](#).

Please note that technical editing may introduce minor changes to the text and/or graphics, which may alter content. The journal's standard [Terms & Conditions](#) and the [Ethical guidelines](#) still apply. In no event shall the Royal Society of Chemistry be held responsible for any errors or omissions in this *Accepted Manuscript* or any consequences arising from the use of any information it contains.



## ARTICLE

# Conjugation-induced fluorescent labelling of mesoporous silica nanoparticles for the sensitive and selective detection of copper ions in aqueous solution

Cite this: DOI: 10.1039/x0xx00000x

Received 00th January 2014,  
Accepted 00th January 2014

DOI: 10.1039/x0xx00000x

www.rsc.org/

Jingjing Cui, Shangfeng Wang, Kai Huang, Yongsheng Li, Wenru Zhao, Jianlin Shi and Jinlou Gu\*

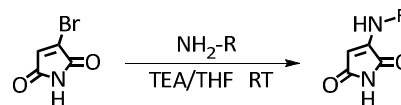
Although the development of sensors for the detection of  $\text{Cu}^{2+}$  ions has significant importance, the sensitive and selective recognition system is still limited. Herein, the non-fluorescent small molecule of 2-bromomaleimide (BM) was firstly converted to 2-aminomaleimide (NM) by a simple nucleophilic addition/elimination reaction with pre-grafted amino groups in meso-space of mesoporous silica nanoparticles (MSNs), and then was designed as fluorescent “on-off” probes for  $\text{Cu}^{2+}$  ion recognition. The strong green fluorescence emitted from pendent NM was induced by the interaction between the lone electron pairs of the N atoms in amino groups and the conjugated maleimide rings. The fluorescence of MSNs labelled NM (MSNs-NM) could be selectively quenched by  $\text{Cu}^{2+}$  in aqueous solution and consequently exhibited sensitive fluorescent “on-off” switching effects for  $\text{Cu}^{2+}$  ions. The detection limit was as low as  $0.28 \mu\text{M}$   $\text{Cu}^{2+}$ , which was far below the U.S. EPA limit of  $20 \mu\text{M}$ . This prefigured the potential applications of the current chemosensor for the detection of  $\text{Cu}^{2+}$  in aqueous solution and in living cells. The small-angle XRD, TEM, BET, FT-IR, UV-Vis absorption measurements all agreed on the fact that the sensitive probes of BM had been successfully labelled into the pore surface of MSNs.

## 1. Introduction

The copper ion is a significant environmental pollutant and also plays a critical role in various biological processes.<sup>1,2</sup> The excess quantities of  $\text{Cu}^{2+}$  can be toxic to biological systems, and cause a series of severe diseases such as Alzheimer's and Wilson's diseases.<sup>3,4</sup> Therefore, the development of sensors for the detection of  $\text{Cu}^{2+}$  ions is of great significance.<sup>5-9</sup> Recently, the fluorescence technique for detecting heavy metal ions has attracted wide attention due to its exquisite sensitivity and selectivity, cost-effectiveness, and superb spatial and temporal resolutions.<sup>10,11</sup> So far, numerous fluorescent chemosensors for heavy metal ions have been developed, which mainly based on small molecular fluorophore, polymer and inorganic nanoparticle.<sup>12-25</sup> Among them, most of the sensors are utilized in homogeneous detection, which critically affects their recycling. In recent years, many efforts have been devoted to the design of organic-inorganic hybrid heterogeneous materials for ion recognition and sensing.<sup>26-30</sup>

As one of the most attractive organic-inorganic hybrid nanomaterials, mesoporous silica nanoparticles (MSNs) appear to be good sensing materials in the heterogeneous solid-liquid

phase due to their large surface area and homogeneous porosity, easy-preparation and functionalization.<sup>31-35</sup> Encapsulation of organic fluorophores in MSNs as optical sensitive probes has attracted a great deal of attention because it features with selective, sensitive and rapid response properties.<sup>36-46</sup> However, the fluorescent MSNs previously reported commonly take several disadvantages such as complicated fluorophores synthesis procedures and harsh fluorophores grafting conditions.



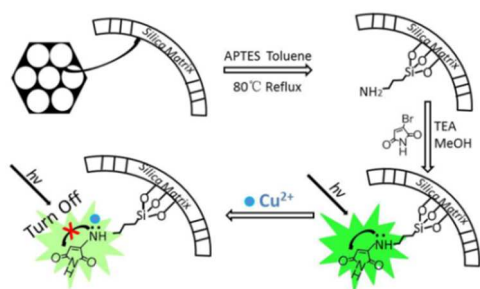
**Scheme 1.** Conversion of small molecule of BM to NM by a nucleophilic addition/elimination reaction with the grafted amino groups within the mesochannels of MSNs under mild reaction condition.

We serendipitously noticed that a simple small molecule of 2-bromomaleimide (BM) had been previously reported as a



novel protein label.<sup>47,48</sup> Although the free BM molecule is non-fluorescent, it was discovered by K. O'Reilly that the strong fluorescence of dithiolmaleimide (DTM) was resulted from the interaction between the lone electron pairs of the S atoms in a protein molecule and the conjugated maleimide rings.<sup>49</sup> These strongly inspired us to explore whether this non-fluorescent small molecule would also become fluorescent upon its introducing into the mesochannels of MSNs if the nucleophilic groups were pre-grafted for its conjugation.

In the current work, the small molecule of BM was converted to 2-aminomaleimide (NM) by a simple nucleophilic addition/elimination reaction with pre-grafted amino groups under mild reaction condition (Scheme 1).<sup>47,50</sup> As expected, the strong green fluorescence emitted from pendent NM was induced by this conjugation although free BM was non-fluorescent. Since the metallic ions could coordinate with the imine groups and consequently mediated their electron donor ability, fluorescent intensity of BM would be facily tuned dependent on the different affinities between the metal ions and nucleophilic groups (Scheme 2).<sup>19,24</sup> We found that the obtained chemosensor exhibited sensitive fluorescent "on-off" switching effects for  $\text{Cu}^{2+}$  via grafted BM on ordered MSNs. The fluorescence of MSNs labelled with BM (MSNs-NM) could be selectively quenched by  $\text{Cu}^{2+}$  in aqueous solution at pH 7.4, and the detection limit was 0.28  $\mu\text{M}$ , which prefigured their potential application for the detection of  $\text{Cu}^{2+}$  in aqueous solution and in living cells.



**Scheme 2.** The schematic presentation of the proposed synthetic routes for BM conjugation into the pore channels of MSNs, and the illustration of the fluorescence emission and quenching mechanism.

## 2. Experimental

### 2.1 Materials

Maleimide, aminopropyltriethoxysilane (3-APTES) and N,N-dimethylhexadecylamine (DHMA) were purchased from Sigma-Aldrich and used as received. All other reagents and chemicals including metals salts were of analytical grade and used as purchased from Sinopharm. Chemical Reagent Co., Ltd without further purification.

### 2.2 Synthesis

**2-Bromomaleimide (BM):** To a solution of maleimide (2.0 g, 20 mmol) in  $\text{CHCl}_3$  was added dropwise a solution of bromine

(1.2 mL, 20 mmol) in  $\text{CHCl}_3$  over 1 h. The reaction mixture was refluxed for 4 h, and then filtered. The yellow solid was washed with cold chloroform for several times to afford crude 2,3-dibromosuccinimide (5.0 g, 19 mmol). The crude product was dissolved in THF (50 mL), and then 10 mL THF with TEA (3.0 mL, 21 mmol) dissolved was added dropwise into the above solution at 0 °C. The resultant mixture was stirred at room temperature for 2 days. The solution was filtered, and the obtained filtrate was concentrated and further purified by silica gel column chromatography using EtOAc/petroleum (1:5, v/v) as the eluent. After drying in a vacuum oven at room temperature, a pale yellow solid of BM was achieved (yield: 2.6 g, 76%).  $^1\text{H}$  NMR (400MHz,  $\text{CDCl}_3$ , Fig. S1):  $\delta$  = 7.61 (br s, 1H, NH),  $\delta$  = 6.88 (s, 1H, C=CH).

**Mesoporous silica nanoparticles (MSNs):** The MSNs was synthesized based on our previous report.<sup>51</sup> As a typical procedure, a given amount of F127 and DHMA were mixed with the structure directing agent of cetyltrimethylammonium bromide (CTAB) in a beaker, and then distilled water was poured into the mixture. Subsequently, sodium hydroxide (2 M, 3.5 mL) solution was added into above mixture under stirring. After a clear and homogeneous solution was formed under constant stirring at 80 °C, TEOS (5.0 mL, 22 mmol) was added dropwise to the above reaction mixture. The temperature was maintained at 80 °C for 2 h. Then the resulting white colloidal suspensions were cooled to room temperature spontaneously. The white colloids were separated by centrifugation with 10,000 rpm for 15 min. and washed with ethanol. The molar composition of the reaction mixture was 8.15 : 0.216 : 0.00289 : 1 : 2.55 : 9700 TEOS : DMHA : F127 : CTAB : NaOH :  $\text{H}_2\text{O}$ . The surfactant of CTAB was extracted by adding 100 mL of ethanol with a little concentrated HCl (12 M, 1.0 mL) mixed into 1.0 g of the resultant MSNs, and refluxed for 24 h under 80 °C.

**Amino groups functionalized mesoporous silica nanoparticles (MSNs- $\text{NH}_2$ ):** The procedure for the modification of the MSNs with amino group was the same to our reported work.<sup>52</sup> Typically, the synthesized MSNs (1.0 g) were suspended in dry toluene (100.0 mL), and aminopropyltriethoxysilane (3-APTES, 1.2 mL) were subsequently administrated. The mixture was stirred at 80 °C for 12 h under  $\text{N}_2$  atmosphere. The resultant white solid of aminopropyl-functionalized MSNs (MSNs- $\text{NH}_2$ ) were centrifuged, washed repeatedly with ethanol. The product was finally dried at 60 °C overnight.

**2-Aminomaleimide moieties functionalized mesoporous silica nanoparticles (MSNs-NM):** In a round-bottomed flask, MSNs-NM (150.0 mg) were suspended in 20 mL of methanol. To this suspension, BM (80.0 mg, 0.45 mmol) and TEA (75.0  $\mu\text{L}$ , 0.54 mmol) were added. The mixture was stirred at room temperature overnight. After centrifugation, the obtained yellow solid (MSNs-NM) was washed repeatedly with methanol and  $\text{H}_2\text{O}$ . After drying at 60 °C overnight, the final yellow powder was achieved.



### 2.3 Fluorescence and UV-vis studies for metal ion detection

The suspension of MSNs-NM ( $30.0 \text{ mg L}^{-1}$ ) was prepared in a 50 mM HEPES buffer solution at pH 7.4. The cation stock solutions were prepared by dissolving the metal salts ( $\text{NaCl}$ ,  $\text{KCl}$ ,  $\text{CaCl}_2$ ,  $\text{MgSO}_4$ ,  $\text{Cu(NO}_3)_2$ ,  $\text{Co(NO}_3)_2$ ,  $\text{Cd(NO}_3)_2$ ,  $\text{Mn(NO}_3)_2$ ,  $\text{Ni(NO}_3)_2$ ,  $\text{AgNO}_3$ ,  $\text{Zn(NO}_3)_2$ ,  $\text{Fe(NO}_3)_3$ ) in deionized water with a concentration of 0.1 M and were diluted as required before use. Each time, 3.0 mL of dispersion solution of MSNs-NM was firstly filled into a quartz cell of 1 cm optical path length, and then added an appropriate concentration and amount of metal ions to the solution for fluorometric and UV-vis measurements. All fluorescence spectra were recorded at room temperature with an excitation wavelength of 371 nm.

### 2.4 Characterization and measurements

X-ray diffraction (XRD) patterns were collected with Bruker D8 using Cu K $\alpha$  radiation (40 kV, 40 mA) at a rate of  $0.6^\circ \text{ min}^{-1}$  over the range of  $0.6\text{--}6^\circ$  ( $2\theta$ ). Transmission electron microscopy (TEM) was conducted on a JEM 2100F electron microscope operated at 200 kV.  $\text{N}_2$  adsorption desorption isotherms were obtained on NOVA 4200E at 77 K under a continuous adsorption condition. Prior to the measurements, all samples were pre-treated for 12 h at  $120^\circ \text{C}$  under nitrogen. The Brunauer-Emmett-Teller (BET) method was utilized to calculate the specific surface areas using adsorption data in a relative pressure range from 0.1 to 0.3. By using the Barrett-Joyner-Halenda (BJH) model, the pore volumes and pore size distributions were derived from the adsorption branches of isotherms, and the total pore volumes were estimated from the adsorbed amount at a relative pressure  $P/P_0$  of 0.99. UV-Visible absorption spectra were recorded on a Shimadzu UV-Vis 3101 spectroscopy. FTIR spectra were recorded on a Nicolet 7000-C spectroscopy with a resolution of  $4 \text{ cm}^{-1}$  using the KBr method. The fluorescence intensity spectra were collected by a Shimadzu RF5301pc fluoro-photometer.  $^1\text{H}$  NMR measurement was carried out on a Bruker AV400 Spectrophotometer. Thermogravimetric analysis (TGA) was conducted on a Perkin-Elmer thermogravimetric analyzer in air ( $50 \text{ mL min}^{-1}$ ) at  $10^\circ \text{C min}^{-1}$  from 30 to  $800^\circ \text{C}$ .

## 3. Results and discussion

### 3.1 Preparation and characterizations of the chemosensor

In this study, we designed a novel chemosensor based on MSNs containing NM for the fluorescence sensing of  $\text{Cu}^{2+}$  ions. MSNs-NM was prepared by a simple nucleophilic addition/elimination reaction between the non-fluorescent small molecule of BM and pre-grafted amino groups in meso-space of MSNs. The performance of MSNs-NM was evaluated for the sensitivity and selectivity towards  $\text{Cu}^{2+}$  ions detection in aqueous media using fluorometric techniques.

The small-angle XRD was applied to monitor the meso-structure evolution for the BM grafting procedures. As manifested in Fig. 1, three distinct diffraction peaks indexed to

(100), (110) and (200) reflections, respectively, could be clearly identified, characterizing their ordered 2D hexagonal ( $P6mm$ ) symmetry. All the diffraction peaks for MSNs- $\text{NH}_2$  (Fig. 1b) and MSNs-NM (Fig. 1c) slightly shifted to higher angle direction. Additionally, the intensities of (110) and (200) reflections also slightly decreased after amino groups and subsequent BM grafting. This peak intensity change was tentatively ascribed to the decreased electron contrast between silica framework and pore channels with organic groups therein in reasonably consistent with our previous observations,<sup>53</sup> evidencing the grafting was successfully done and took place inside the mesoporous channels.

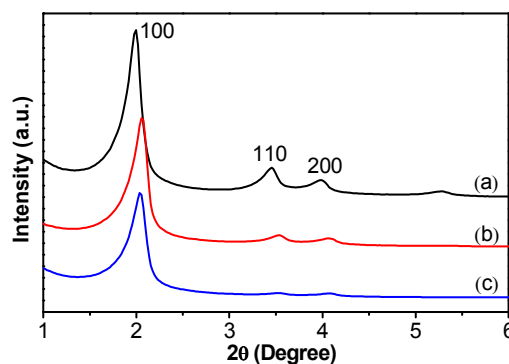


**Fig. 1** Small-angle XRD patterns of the synthesized (a) MSNs, (b) MSNs- $\text{NH}_2$  and (c) MSNs-NM.

TEM images were taken to directly observe the morphology of the synthesized samples. The parent MSNs (Fig. 2a) exhibited the very uniform spherical shape with diameter of about 155 nm (Also see the Fig. S2). After modification, the morphology of MSNs-NM was preserved. The parallel mesopore channels penetrated throughout the whole nanoparticles. Meanwhile, hexagonally arranged mesochannels were present as shown in Fig. 2 (b), corroborating that the prepared sample possessed a well-ordered mesostructure and the BM grafting did not affect the general morphology of MSNs. Thus, from the TEM image analysis and the small-angle XRD patterns, it can be concluded that the ordered mesoporous silica-based matrix remains intact throughout the modification steps.

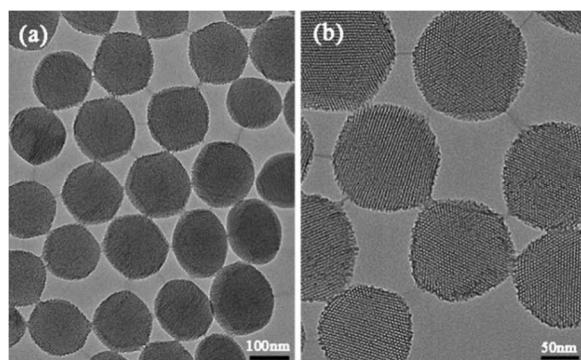


**Fig. 2** TEM images of the synthesized (a) MSNs and (b) MSNs-NM.



The changes of the textural parameters of the MSNs before and after the BM grafting were further investigated by nitrogen sorption technique. The nitrogen adsorption curves (Fig. 3A) revealed type-IV isotherms with sharp capillary condensation steps for all the samples before and after BM grafting. This evidences the presence of mesoporous structure in these materials and also indicates that the modification process did not destroy the structural integrity of the parent MSNs. The sharp increase in  $N_2$  uptake of parent MSNs (Fig. 3a) is observed at a relative pressure of 0.3-0.5, clearly indicating that the mesopores are uniform in size. Meanwhile, the capillary condensation steps shifted to a relatively lower pressure after amino groups and subsequent BM modification. This illustrates the successful attachment of BM to the void space of the MSNs, which causes the shrinkage of the pore volume as well as the decrease of the specific surface area of the modified materials (Table 1). The pore size distributions calculated by BJH method (Fig. 3B) clearly reflects a decrease in pore size. The gradual decrease in pore width from 3.10 to 2.75 and to 2.46 nm also suggests that the BM were successfully grafted inside the MSNs.

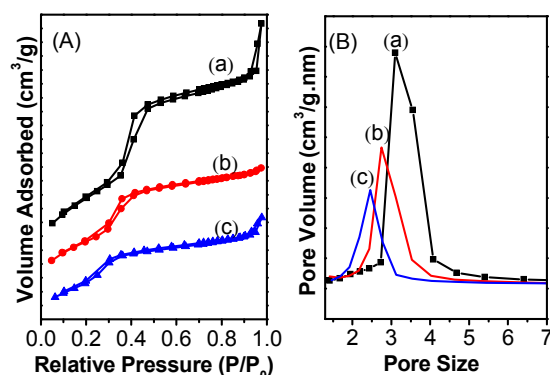


**Fig. 3**  $N_2$  adsorption-desorption isotherms (A) and their corresponding BJH pore size distribution curves (B) of the samples for (a) MSNs, (b) MSNs-NH<sub>2</sub> and (c) MSNs-NM.

**Table 1.** The structural parameters of the MSNs before and after the BM grafting

Samples	$S_{BET}$ (m <sup>2</sup> g <sup>-1</sup> )	$D_{BJH}$ (nm)	$V$ (cm <sup>3</sup> g <sup>-1</sup> )
MSNs	1481	3.10	1.55
MSNs-NH <sub>2</sub>	1099	2.75	0.83
MSNs-NM	871	2.46	0.70

To further testify the successful labelling of the MSNs with fluorescent probes, the FT-IR spectra were taken to trace the grafting procedures. As shown in Fig. 4, the reduced IR absorption of C-H bonds at 2900-3000 cm<sup>-1</sup> after the extraction using ethanol and concentrated HCl (Fig. 4a) indicated that the surfactant had been effectively removed from the MSNs. An apparent intensity decrease of the Si-OH vibration bands at 960 cm<sup>-1</sup> can be observed while the new -CH<sub>2</sub>-NH<sub>2</sub> mode at 1552 cm<sup>-1</sup> (labelled with arrow) and C-H bonds at 2900-3000 cm<sup>-1</sup> (Fig. 4b) for propyl groups in APTES emerge in MSNs-NH<sub>2</sub>,

clearly verifying the successful incorporation of the amino groups. The band occurred at 1708 and 1760 cm<sup>-1</sup> (labelled with stars) for MSNs-NM (Fig. 4c) could be assigned to the five membered rings of imide.<sup>54</sup> These results indicated that BM had been attached to the amino groups. We can also confirm the successful linking of fluorescent probes from the UV-vis measurement. The spectrum (Fig. S3) of MNS-NMs exhibits a new absorption band at 371 nm arising from BM while parent and amino groups modified MSNs do not show any absorption at the same bands. TGA measurement illustrates that the loading capacity of the fluorescent probe on the synthesized chemosensor was determined to be 0.1 g per gram of MSNs (Fig. S4).

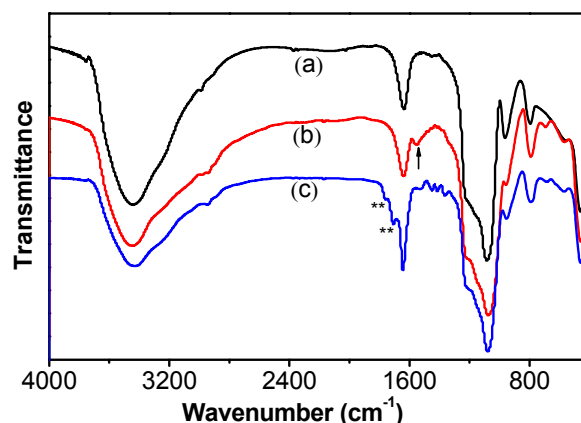


**Fig. 4** FT-IR spectra the synthesized (a) MSNs, (b) MSNs-NH<sub>2</sub> and (c) MSNs-NM.

### 3.2 Selectivity of the MSNs-NM towards Cu<sup>2+</sup> ions

To check whether the MSNs-NM could serve as fluorogenic sensors for metallic ions, we tested the fluorescence response of MSNs-NM towards various metal ions such as Cu<sup>2+</sup>, Fe<sup>3+</sup>, Co<sup>2+</sup>, Zn<sup>2+</sup>, Ag<sup>+</sup>, Ni<sup>2+</sup>, Mn<sup>2+</sup>, Cd<sup>2+</sup>, Mg<sup>2+</sup>, Ca<sup>2+</sup>, K<sup>+</sup> and Na<sup>+</sup>. The fluorescence response was recorded at 505 nm following by excitation at 371 nm in HEPES buffer solution (50 mM, pH = 7.4). Fig. 5 illustrate the quenching ratio, ((F<sub>0</sub>-F)/F<sub>0</sub>), of fluorescence intensity upon addition of 150 μM various metal ions to MSNs-NM suspension (30 mg L<sup>-1</sup>). The results show that no obvious changes occurred in the presence of alkali and alkaline earth metal ions (Na<sup>+</sup>, K<sup>+</sup>, Mg<sup>2+</sup>, Ca<sup>2+</sup>), or transition ions (Cd<sup>2+</sup>, Zn<sup>2+</sup>, Co<sup>2+</sup>, Ni<sup>2+</sup>, Ag<sup>+</sup>) except that Fe<sup>3+</sup> caused a slight fluorescence decrease. However, it was found the fluorescence intensity decreased dramatically to 34% upon the addition of Cu<sup>2+</sup> to the suspension. These results reveal that MSNs-NM exhibit high selectivity and sensibility towards Cu<sup>2+</sup> ions in aqueous solution as we expected (See Fig. S5 for the corresponding fluorescence spectra). Since the high specificity is crucial for most probes to be applied in the real sample detection, we further added other metallic ions to the MSNs-NM-Cu<sup>2+</sup> system. No significant fluorescence intensity changes were observed in the experiments in which other metal ions were spontaneously added into the Cu<sup>2+</sup>-containing detecting systems (Fig. S6). These findings confirm that the current



obtained MSNs-NM can be useful for the selective detection of  $\text{Cu}^{2+}$  in the presence of other metal ions.

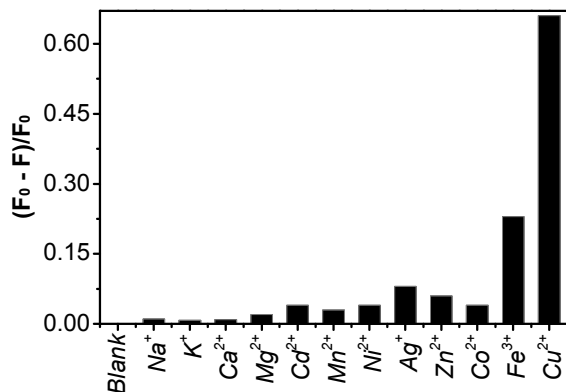


**Fig. 5** Quenching ratio  $((F_0-F)/F_0)$  of fluorescence response of MSNs-NM suspension ( $30 \text{ mg L}^{-1}$ ) in HEPES solution ( $50 \text{ mM}$ ;  $\text{pH} = 7.4$ ) in the presence of various metal ions ( $150 \text{ }\mu\text{M}$ ) ( $\lambda_{\text{ex}} = 371 \text{ nm}$ ,  $\lambda_{\text{em}} = 505 \text{ nm}$ ).

### 3.3 Sensing response of MSNs-NM towards $\text{Cu}^{2+}$ ions

To test the sensibility of MSNs-NM for  $\text{Cu}^{2+}$ , fluorescence titration spectra with different  $\text{Cu}^{2+}$  concentration were conducted following by excitation at  $371 \text{ nm}$  at room temperature. Upon gradual addition of  $\text{Cu}^{2+}$  ions (from  $0$  to  $150 \text{ }\mu\text{M}$ ) to the MSNs-NM suspension, it was found that the fluorescence intensity was dramatically decreased (Fig. 6), confirming their potentials for the  $\text{Cu}^{2+}$  detection. The response time of the fluorescent probe to the  $\text{Cu}^{2+}$  ions was also detected (Fig. S7), and the calculated value was as short as  $75$  seconds, which was much faster than those of the reported work.<sup>55,56</sup> Therefore, a reaction time of  $90$  seconds was set to ensure the complete equilibration before measurement for all the experiments.

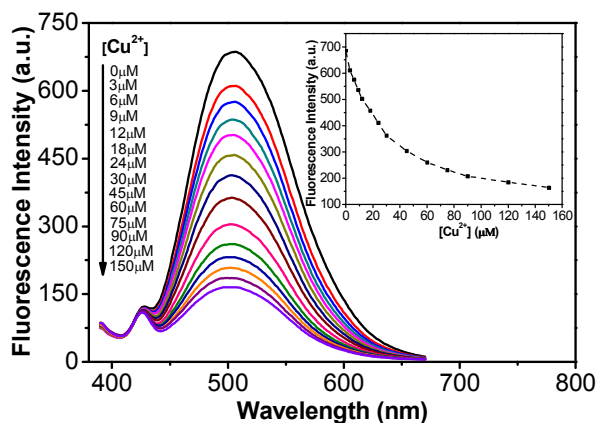


**Fig. 6** Fluorescence spectra of MSNs-NM suspension ( $30 \text{ mg L}^{-1}$ ) in a HEPES solution ( $50 \text{ mM}$ ;  $\text{pH} = 7.4$ ) in the presence of different amounts of  $\text{Cu}^{2+}$  (from  $0$  to  $150 \text{ }\mu\text{M}$ ). Inset: the fluorescence intensity at  $505 \text{ nm}$  as a function of  $\text{Cu}^{2+}$  ions concentration. Excitation wavelength was set at  $371 \text{ nm}$ .

Quenching of fluorescence is described by the Stern-Volmer equation<sup>57</sup> (equation 1):

$$\frac{F_0}{F} = 1 + K_{sv}[Q] \quad (1)$$

In this equation  $F_0$  and  $F$  are the fluorescence intensities of MSNs-NM in the absence and presence of  $\text{Cu}^{2+}$ , respectively;  $Q$  is the concentration of  $\text{Cu}^{2+}$ , and  $K_{sv}$  is Stern-Volmer quenching constant. Fig. 7 shows the plot of  $F_0/F$  versus  $[\text{Cu}^{2+}]$  with a good linear relationship between relative fluorescence intensity and  $\text{Cu}^{2+}$  concentration at the range from  $0$  to  $90 \text{ }\mu\text{M}$ , following the equation  $F_0/F = 0.26 \times 10^5 [\text{Cu}^{2+}] + 1.05$  with linearly dependent coefficient  $r^2 = 0.997$ . The  $K_{sv}$  is determined to be  $2.6 \times 10^4 \text{ M}^{-1}$ . When the  $\text{Cu}^{2+}$  concentration exceeds  $90 \text{ }\mu\text{M}$ , the Stern-Volmer plots deviate from linearity toward the x-axis. This maybe attributes to the partial inaccessibility of the fluorescent probes to the  $\text{Cu}^{2+}$  ions in the mesopores space of MSNs. This also rationalizes that the fluorescence intensity of MSNs-NM is not completely quenched by the addition of  $\text{Cu}^{2+}$  ions.

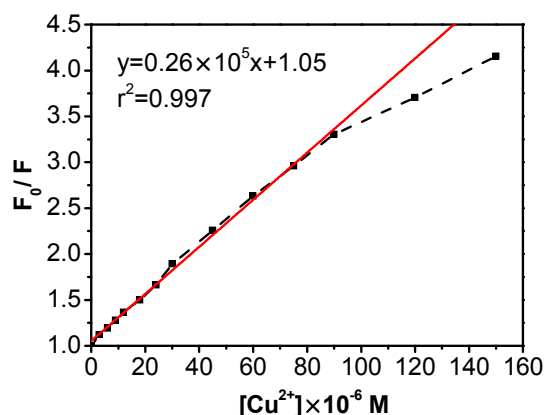


**Fig. 7** Stern-Volmer plot of MSNs-NM suspension ( $30 \text{ mg L}^{-1}$ ) in a HEPES solution ( $50 \text{ mM}$ ;  $\text{pH} = 7.4$ ) in the presence of different amounts of  $\text{Cu}^{2+}$  ions (from  $0$  to  $150 \text{ }\mu\text{M}$ ) ( $\lambda_{\text{ex}} = 371 \text{ nm}$ ,  $\lambda_{\text{em}} = 505 \text{ nm}$ ).

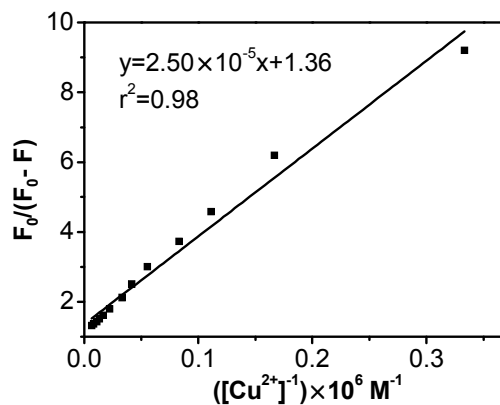


**Fig. 8** Modified Stern-Volmer plot of MSNs-NM suspension ( $30 \text{ mg L}^{-1}$ ) in a HEPES solution ( $50 \text{ mM}$ ;  $\text{pH} = 7.4$ ) in the



presence of different amounts of  $\text{Cu}^{2+}$  ions (from 0 to 150  $\mu\text{M}$ ) ( $\lambda_{\text{ex}} = 371 \text{ nm}$ ,  $\lambda_{\text{em}} = 505 \text{ nm}$ ).

The modified Stern-Volmer equation (equation 2)<sup>58</sup> is applied for quantitative evaluation of the accessible fraction of fluorescence molecules.

$$\frac{F_0}{F_0 - F} = \frac{1}{f_a K_a [Q]} + \frac{1}{f_a} \quad (2)$$

Where  $f_a$  is the fraction of initial fluorescence that is accessible to quencher and  $K_a$  is Stern-Volmer quencher constant of the accessible fraction. This modified form of the Stern-Volmer equation allows  $f_a$  and  $K_a$  to be determined graphically (Fig. 8). A plot of  $F_0/(F_0 - F)$  versus  $1/[Q]$  yields  $f_a^{-1}$  as the intercept and  $(f_a K_a)^{-1}$  as the slope. Thus,  $K_a$  is calculated to be  $5.41 \text{ M}^{-1}$  and  $f_a$  is obtained as 0.73, revealing that almost 73% of the MSNs-NM are accessible to  $\text{Cu}^{2+}$  ions. It can be taken into account as the rationalized reason for the remaining observed fluorescence.

The detection limit (DL) was calculated from equation 3:

$$DL = \frac{3\sigma}{m} \quad (3)$$

Where  $\sigma$  is standard deviation of the blank measurements, and  $m$  is the slope of  $F-[\text{Cu}^{2+}]$  plot with the concentrations of  $\text{Cu}^{2+}$  in the range from 0 to 30  $\mu\text{M}$ . Herein,  $\sigma$  and  $m$  are calculated to be 2.84 and  $9.97 \times 10^6$ , respectively. Then the detection limit is calculated to be 0.28  $\mu\text{M}$ , which is more than sufficient to sense the  $\text{Cu}^{2+}$  concentration in drinking water with respect to the U.S. EPA limit ( $\approx 20 \mu\text{M}$ ).<sup>59</sup>

### 3.4 Possible sensing mechanism

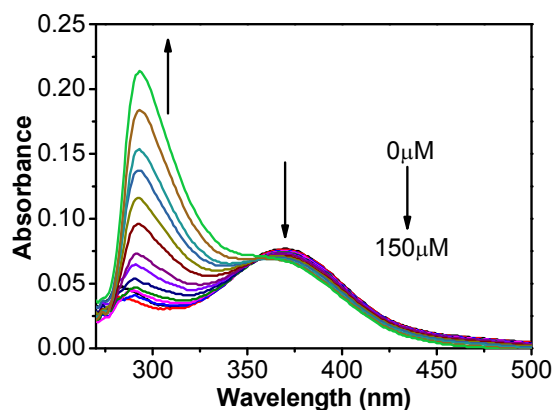


**Fig. 9** The absorption spectra of MSNs-NM suspension ( $30 \text{ mg L}^{-1}$ ) in the presence of different amounts of  $\text{Cu}^{2+}$  ions (from 0 to 150  $\mu\text{M}$ ) in a HEPES solution (50 mM; pH = 7.4).

To explore the mechanism of the fluorescence quenching by the  $\text{Cu}^{2+}$  ions, we further tested the UV-vis absorption of the current conjugated system. Fig. 9 shows the spectral variation of MSNs-NM suspension ( $30 \text{ mg L}^{-1}$ ) in a HEPES solution upon the gradual addition of  $\text{Cu}^{2+}$  ions. It is observed that free MSNs-NM shows an absorbance maximum at 371 nm. When

$\text{Cu}^{2+}$  ions were introduced, a new absorption band peaked at 293 nm was observed while the intensity of 371 nm was decreased. A clear isosbestic point at 356 nm was observed simultaneously, indicating the conversion of NM to  $\text{Cu}^{2+}$ -NM complexes. This observation can be considered as a reason for fluorescence quenching. It reveals that the low energy band still exists but the intensity slightly decreases, and a new high energy band forms.

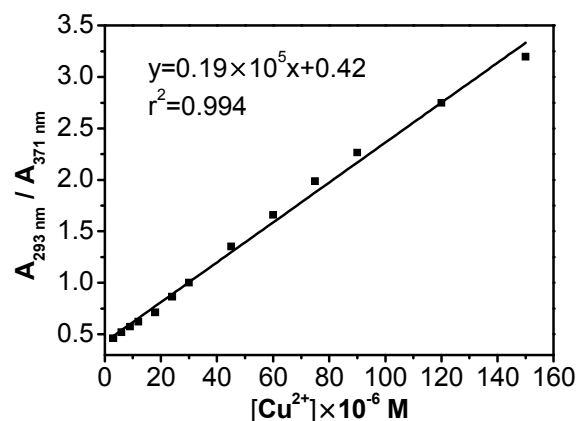


**Fig. 10** The absorption ratios ( $A_{293 \text{ nm}}/A_{371 \text{ nm}}$ ) of MSNs-NM suspension ( $30 \text{ mg L}^{-1}$ ) in the presence of different amounts of  $\text{Cu}^{2+}$  ions (from 0 to 150  $\mu\text{M}$ ) in a HEPES solution (50 mM; pH = 7.4).

Fig. 10 shows the UV-vis absorption intensity ratios, which were measured at 293 and 371 nm, respectively. It shows a good linear relationship between absorption intensity ratios and  $\text{Cu}^{2+}$  concentration. This indicates that MSNs-NM not only could serve as fluorogenic sensors but also has the potentials for quantitative determination of  $\text{Cu}^{2+}$  ions even using UV-Vis analytical method.<sup>3</sup>

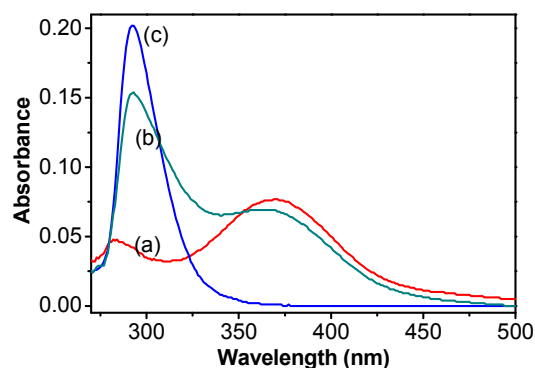


**Fig. 11** The absorption spectra of MSNs-NM suspension ( $30 \text{ mg L}^{-1}$ , a, red), MSNs-NM- $\text{Cu}^{2+}$  suspension ( $90 \mu\text{M} \text{ Cu}^{2+}$ , b, green) and free maleimide ( $50 \mu\text{M}$ , c, blue) in a HEPES solution (50 mM; pH = 7.4).



To provide the direct proof of the coordination between MSNs-NM and  $\text{Cu}^{2+}$ , we measured the UV-Vis spectra of free maleimide and compared it with the spectra of MSNs-NM and MSNs-NM- $\text{Cu}^{2+}$ . As shown in Fig. 11, the spectrum of free maleimide shows an obvious absorption band at 292 nm, while a new absorption band centred at 371 nm appears and it becomes fluorescent when maleimide is conjugated to the MSNs *via* amino groups. When  $\text{Cu}^{2+}$  ions are added, the lone electron pairs of N atoms are strictly restricted by  $\text{Cu}^{2+}$  due to their strong interaction, so the absorption band of maleimide is partially recovered (Fig. 11b). The more  $\text{Cu}^{2+}$  ions are introduced, the more intense absorption at 292 nm assigned to free maleimide is recovered (Fig. 9) and thus causes the fluorescence quenching and absorption change of the conjugated BM molecules.

#### 4. Conclusions

In summary, a novel fluorescent “on-off” chemosensor for  $\text{Cu}^{2+}$  ions has been successfully developed *via* labelling mesoporous silica nanoparticles (MSNs) with maleimide. Although the free maleimide molecule is non-fluorescent, the introduction of this small molecule into the mesochannels of MSNs makes them fluorescent thanks to the nucleophilic amino groups for their conjugation.  $\text{N}_2$  sorption analysis, FT-IR and UV-Vis spectra revealed that maleimide was successfully grafted to the mesopores. Small-angle XRD and TEM data suggested that the highly ordered mesoporous structure was retained after all processes for the sensor fabrication. The new chemosensor presents a high selectivity toward  $\text{Cu}^{2+}$  than other metal ions with detection limit as low as 0.28  $\mu\text{M}$ . Additionally, the synthesized MSNs-NM not only could serve as fluorogenic sensors but also has the potentials for quantitative determination of  $\text{Cu}^{2+}$  even using chromogenic method. A rationalized mechanism for fluorescence quenching was proposed that the strong interaction between amino groups of 2-aminomaleimides and  $\text{Cu}^{2+}$  ions restricted the lone electron pairs of N atoms to conjugate with the maleimide ring. The above sensor system is expected to be used for the detection of  $\text{Cu}^{2+}$  in intercellular environments and water-quality monitoring.

#### Acknowledgements

This work was financially supported by the Natural Science Foundation of China (51372084, 51072053), the Innovation Program of Shanghai Municipal Education Commission (13zz040), the Nano-Special Foundation for Shanghai Committee of Science and Technology (12nm0502600) and the 111 Project (B14018).

#### Notes and references

Key Laboratory for Ultrafine Materials of Ministry of Education, School of Materials Science and Engineering, East China University of Science and Technology, Shanghai 200237, China. E-mail: jinlougu@ecust.edu.cn; Fax: +86-21-64250740; Tel: +86-21-64252599

†Electronic Supplementary Information (ESI) available: [NMR of the BM, TEM image and the particle size distribution histogram, UV-vis, TGA, fluorescence measurement, fluorescence response curves and time titration profile]. See DOI: 10.1039/b000000x/

- 1 Y. W. Liu, J. L. Chir, S. T. Wang and A. T. Wu, *Inorg. Chem. Commun.*, 2014, **45**, 112.
- 2 E. L. Que, D. W. Domaille and C. J. Chang, *Chem. Rev.*, 2008, **108**, 1517.
- 3 H. H. Wang, L. X. Zhang, J. F. Guo, P. Li and H. Jiang, *New J. Chem.*, 2010, **34**, 1239.
- 4 S. D. R. Brown and H. Kozłowski, *Dalton Trans.*, 2004, **13**, 1907.
- 5 B. F. Gouanvé, T. Schuster, E. Allard, R. Méallet-Renault and C. Larpent, *Adv. Funct. Mater.*, 2007, **17**, 2746.
- 6 K. Viswanathan, *Sensors and Actuators A*, 2012, **175**, 15.
- 7 P. Yang, Y. Zhao, Y. Lu, Q. Z. Xu, X. W. Xu, L. Dong and S. H. Yu, *ACS Nano*, 2011, **5**, 2147.
- 8 C. Yu, J. Zhang, R. Wang and L. X. Chen, *Org. Biomol. Chem.*, 2010, **8**, 5277.
- 9 C. Yu, L. X. Chen, J. Zhang, J. H. Li, P. Liu, W. H. Wang and B. Yan, *Talanta*, 2011, **85**, 1627.
- 10 H. N. Kim, M. H. Lee, H. J. Kim, J. S. Kim and J. Yoon, *Chem. Soc. Rev.*, 2008, **37**, 1465.
- 11 T. Balaji, S. A. El-Safty, H. Matsunaga, T. Hanaoka and F. Mizukami, *Angew. Chem. Int. Ed.*, 2006, **45**, 7202.
- 12 K. Singh, D. Sareen, P. Kaur, H. Miyake and H. Tsukube, *Chem. Euro. J.*, 2013, **19**, 6914.
- 13 L. Prodi, *New J. Chem.*, 2005, **29**, 20.
- 14 Y. Xiang, A. Tong, P. Jin and Y. Ju, *Org. Lett.*, 2006, **8**, 2863.
- 15 C. Bhattacharya, Z. Q. Yu, M. J. Rishel and S. M. Hecht, *Biochemistry*, 2014, **53**, 3264.
- 16 Z. Q. Yu, R. M. Schmaltz, T. C. Bozeman, R. Paul, M. J. Rishel, K. S. Tsosie and S. M. Hecht, *J. Am. Chem. Soc.*, 2013, **135**, 2883.
- 17 Z. Q. Yu, T. Kabashima, C. H. Tang, T. Shibata, K. Kitazato, N. Kobayashi, M. K. Lee and M. Kai, *Anal. Biochem.*, 2010, **397**, 197.
- 18 T. Kabashima, Z. Q. Yu, C. H. Tang, Y. Nakagawa, K. Okumura, T. Shibata, J. Z. Lu and M. Kai, *Peptides*, 2008, **29**, 356.
- 19 M. Montalti, E. Rampazzo, N. Zaccheroni and L. Prodi, *New J. Chem.*, 2013, **37**, 28.
- 20 J. T. Yeh, W. C. Chen, S. R. Liu and S. P. Wu, *New J. Chem.*, 2014, **38**, 4434.
- 21 G. J. He, X. W. Zhao, X. L. Zhang, H. J. Fan, S. Wu, H. Q. Li, C. He and C. Y. Duan, *New J. Chem.*, 2010, **34**, 1055.
- 22 A. Ajayaghosh, P. Carol and S. Sreejith, *J. Am. Chem. Soc.*, 2005, **127**, 14962.
- 23 G. Zhang, D. Zhang, S. Yin, X. Yang, Z. Shuai and D. Zhu, *Chem. Commun.*, 2005, **16**, 2161.
- 24 X. Qi, E. J. Jun, L. Xu, S.-J. Kim, J. S. Joong Hong, Y. J. Yoon and J. Yoon, *J. Inorg. Chem.*, 2006, **71**, 2881.
- 25 H. Son, G. Kang and J. H. Jung, *Analyst*, 2012, **137**, 163.
- 26 S. J. Lee, S. S. Lee, M. S. Lah, J.-M. Hong and J. H. Jung, *Chem. Commun.*, 2006, **43**, 4539.
- 27 S. J. Lee, J. E. Lee, J. Seo, I. Y. Jeong, S. S. Lee and J. H. Jung, *Adv. Funct. Mater.*, 2007, **17**, 3441.
- 28 X. Qiu, S. Han and M. Gao, *J. Mater. Chem. A*, 2013, **1**, 1319.
- 29 C. Wang, S. Tao, W. Wei, C. Meng, F. Liu and M. Han, *J. Mater. Chem.*, 2010, **20**, 4635.



- 30 X.-C. Fu, J. Wu, C.-G. Xie, Y. Zhong and J.-H. Liu, *Anal. Methods*, 2013, **5**, 2615.
- 31 M. S. Moorthy, H.-J. Cho, E.-J. Yu, Y.-S. Jung and C.-S. Ha, *Chem. Commun.*, 2013, **49**, 8758.
- 32 S. A. El-Safty, A. A. Ismail, H. Matsunaga and F. Mizukami, *Chem. Euro. J.*, 2007, **13**, 9245.
- 33 R. Metivier, I. Leray, B. Lebeau and B. Valeur, *J. Mater. Chem.*, 2005, **15**, 2965.
- 34 D. Lu, L. Yang, Z. Tian, L. Wang and J. Zhang, *RSC Adv.*, 2012, **2**, 2783.
- 35 X. Wan, S. Yao, H. Liu and Y. Yao, *J. Mater. Chem. A*, 2013, **1**, 10505.
- 36 P. Pal, S. K. Rastogi, C. M. Gibson, D. E. Aston, A. L. Branen, and T. E. Bitterwolf, *ACS Appl. Mater. Interfaces*, 2011, **3**, 279.
- 37 Y. Hu, L. Meng and Q. H. Lu, *Langmuir*, 2014, **30**, 4458.
- 38 Z. Jin, X. B. Zhang, D. X. Xie, Y. J. Gong, J. Zhang, X. Chen, G. L. Shen and R. Q. Yu, *Anal. Chem.*, 2010, **82**, 6343.
- 39 H. J. Kim, H. Lee, J. H. Lee, D. H. Choi, J. H. Jung and J. S. Kim, *Chem. Commun.*, 2011, **47**, 10918.
- 40 H. J. Kim, J. H. Lee, H. Lee, J. H. Lee, J. H. Lee, J. H. Jung and J. S. Kim, *Adv. Funct. Mater.*, 2011, **21**, 4035.
- 41 Q. Zou, L. Zou and H. Tian, *J. Mater. Chem.*, 2011, **21**, 14441.
- 42 J. Liu, C. Li and F. Li, *J. Mater. Chem.*, 2011, **21**, 7175.
- 43 K. Sarkar, K. Dhara, M. Nandi, P. Roy, A. Bhaumik and P. Banerjee, *Adv. Funct. Mater.*, 2009, **19**, 223.
- 44 J. Wang, W. Guo, J.-H. Bae, S.-H. Kim, J. Song and C.-S. Ha, *J. Mater. Chem.*, 2012, **22**, 24681.
- 45 H. J. Kim, S. J. Lee, S. Y. Park, J. H. Jung and J. S. Kim, *Adv. Mater.*, 2008, **20**, 3229.
- 46 B. Leng, J. Jiang and H. Tian, *AIChE J.*, 2010, **56**, 2957.
- 47 M. E. B. Smith, F. F. Schumacher, C. P. Ryan, L. M. Tedaldi, D. Papaioannou, G. Waksman, S. Caddick and J. R. Baker, *J. Am. Chem. Soc.*, 2010, **132**, 1960.
- 48 M. W. Jones, R. A. Strickland, F. F. Schumacher, S. Caddick, J. R. Baker, M. I. Gibson and D. M. Haddleton, *J. Am. Chem. Soc.*, 2011, **134**, 1847.
- 49 M. P. Robin, P. Wilson, A. B. Mabire, J. K. Kiviahio, J. E. Raymond, D. M. Haddleton and R. K. O'Reilly, *J. Am. Chem. Soc.*, 2013, **135**, 2875.
- 50 J. L. Gu, S. Su, Y. Li, Q. He and J. Shi, *Chem. Commun.*, 2011, **47**, 2101.
- 51 J. L. Gu, K. Huang, X. Zhu, Y. Li, J. Wei, W. Zhao, C. Liu and J. Shi, *J. Colloid Interf. Sci.*, 2013, **407**, 236.
- 52 J. L. Gu, J. Shi, G. You, L. Xiong, S. Qian, Z. Hua and H. Chen, *Adv. Mater.*, 2005, **17**, 557.
- 53 J. L. Gu, W. Fan, A. Shimojima and T. Okubo, *Small*, 2007, **3**, 1740.
- 54 O. E. Tall, Y. Hou, E. Abou-Hamad, I. U. Raja, M. N. Hedhili, W. Peng, R. Mahfouz, O. M. Bakr and P. M. Beaujuge, *Chem. Mater.*, 2014, **26**, 2766.
- 55 J. F. Zhang, M. S. Park, W. X. Ren, Y. Kim, S. J. Kim, J. H. Jung and J. S. Kim, *Chem. Commun.*, 2011, **47**, 3568.
- 56 A. Lee, J. Chin, O. K. Park, H. Chung, J. W. Kim, S. Y. Yoon and K. Park, *Chem. Commun.*, 2013, **49**, 5969.
- 57 P. Zarabadi-Poor, A. Badiei, A. A. Yousefi and J. Barroso-Flores, *J. Phys. Chem. C.*, 2013, **117**, 9281.
- 58 J. R. Lakowicz, *Principles of Fluorescence Spectroscopy*, Kluwer Acad./Plenum Publ., 1999, pp. 288.
- 59 S. Seo, H. Y. Lee, M. Park, J. M. Lim, D. Kang, J. Yoon and J. H. Jung, *Eur. J. Inorg. Chem.*, 2010, **6**, 843.



## Table of Content (TOC)

### Conjugation-induced fluorescent labelling of mesoporous silica nanoparticles for the sensitive and selective detection of copper ions in aqueous solution

Jingjing Cui, Shangfeng Wang, Kai Huang, Yongsheng Li, Wenru Zhao, Jianlin Shi and Jinlou Gu\*

A newly developed fluorescent “on-off” chemosensor presents a high selectivity towards  $\text{Cu}^{2+}$  with detection limit as low as  $0.28 \mu\text{M}$ .

